

Design and Synthesis of Hierarchical MnO₂ Nanospheres/Carbon Nanotubes/Conducting Polymer Ternary Composite for High Performance Electrochemical Electrodes

Ye Hou,[†] Yingwen Cheng,[†] Tyler Hobson,[‡] and Jie Liu^{*·†}

[†]Department of Chemistry, Duke University, Durham, North Carolina, 27708 and [‡]Riverside High School, 101 East Murray Avenue, Durham, North Carolina, 27704

ABSTRACT For efficient use of metal oxides, such as MnO₂ and RuO₂, in pseudocapacitors and other electrochemical applications, the poor conductivity of the metal oxide is a major problem. To tackle the problem, we have designed a ternary nanocomposite film composed of metal oxide (MnO₂), carbon nanotube (CNT), and conducting polymer (CP). Each component in the MnO₂/CNT/CP film provides unique and critical function to achieve optimized electrochemical properties. The electrochemical performance of the film is evaluated by cyclic voltammetry, and constant-current charge/discharge cycling techniques. Specific capacitance (SC) of the ternary composite electrode can reach 427 F/g. Even at high mass loading and high concentration of MnO₂ (60%), the film still showed SC value as high as 200 F/g. The electrode also exhibited excellent charge/discharge rate and good cycling stability, retaining over 99% of its initial charge after 1000 cycles. The results demonstrated that MnO₂ is effectively utilized with assistance of other components (fFWNTs and poly(3,4-ethylenedioxythiophene)–poly(styrenesulfonate)) in the electrode. Such ternary composite is very promising for the next generation high performance electrochemical supercapacitors.

KEYWORDS MnO₂; fFWNTs; PEDOT–PSS; supercapacitor; effective utilization.

As the limited availability of fossil fuel and the environmental impacts of a society based on such energy sources becoming more obvious, the need for renewable energy sources has attracted attentions of the world. Systems for electrochemical energy storage and conversion include batteries, fuel cells, and supercapacitors. Among them, supercapacitors, also known as electrical double layer capacitor, ultracapacitor, or electrochemical capacitor (EC), have attracted much attention because of their high power density, long cycle life (>100 000 cycles), and rapid charging-discharging rates.¹ They can be applied in a large variety of applications, including consumer electronics, memory back-up systems, industrial power, energy management, public transportation, and military devices. More importantly, supercapacitors are critical components in the next generation all-electric cars and cars based on fuel cells that use hydrogen or alcohol as clean and renewable energy media.

Various materials have been investigated as the electrodes in ECs, including carbonaceous materials,^{2–4} conducting polymers^{5,6} and transition-metal oxides.^{7,8} MnO₂ is generally considered to be the most promising transition metal oxides for the next generation of supercapacitors because of its high-energy density, low cost, environmental friendliness, and natural abundance.^{9,10}

The published results thus far established that the electrochemical performance of MnO₂ depended on their morphology, porosity, specific surface area, electrical conductivity and ionic transport within the pores.^{11,12} In this context, layered mesoporous birnessite-type manganese oxide materials are attracting great interest due to their high surface area, low density, and good permeation.^{13–17} However, the fabrication of birnessite-type manganese oxide architectures remains a significant challenge due to the fast and uncontrolled growth process.^{18,19}

Literature reviews of electrodes made from MnO₂ showed that high specific capacitance and rate capability should be obtained in principle.^{1,20–22} However, a key weakness of the metal oxide material is its limited electric conductivity.²³ To effectively utilize MnO₂ materials, binary composites of hydrous MnO₂ with either carbon nanotubes (CNTs)^{24–29} or conducting polymers^{30–32} have been explored and demonstrated improvement in the electrochemical performance. However, conducting polymers and metal-oxides both suffer from mechanical instability.²³ Electrodes made of hydrous MnO₂ with conducting polymers showed mechanical instability and poor cycleability. For composites with carbonaceous materials, including CNTs, the reported enhancement of electrochemical performance is more pronounced when only a small amount of metal oxide is incorporated in the electrode.³³ However, for practical applications, particularly for large capacitor applications, such as power sources for the hybrid electric vehicle (HEV) or fuel cell electric

* To whom correspondence should be addressed. E-mail: j.liu@duke.edu.

Received for review: 5/16/2010

Published on Web: 06/29/2010

vehicle (FCEV), high metal oxide concentration in electrodes and high mass loading of total active materials are needed. Unfortunately, due to the dense morphology and the intrinsically poor electrical conductivity of MnO_2 , its electrochemical performance is unsatisfactory if the loading of MnO_2 is high. When the weight percentage is increased, MnO_2 becomes densely packed with limited accessible surface area, only a very thin layer of the oxide material participated in the charge storage process, resulting in both high resistance and a comparatively low specific capacitance. These lead to a significant degradation from the theoretical advantages of the material and eventually reduces its attractiveness in future application. Therefore, the low-energy density caused by the limited loading of hydrous MnO_2 still remains a major problem. Extensive efforts are still needed to improve the electrochemical utilization of MnO_2 , especially in the cases where high metal oxide loading is needed.

In the present paper, we report a novel design and synthesis of a ternary $\text{MnO}_2/\text{CNT}/\text{CP}$ composite for high-performance electrochemical electrodes. New insights on the design of an ideal electrochemical capacitor with both high energy and power density are provided. In our approaches, we focus on the synergistic effects from the combination of MnO_2 , functionalized few-walled carbon nanotubes (fFWNTs) grown by chemical vapor deposition method³⁴ (see Supporting Information I) and commercial PEDOT–PSS conducting polymer in the composites to effectively utilize the full potential of all the desired functions of each component. Hence, this composite provides a direction toward solving the potential problems and is very promising for the next generation high-performance electrochemical electrodes.

Looking carefully at the charge storage process, a main existing problem is that the underlying bulk oxide materials remain as dead volume, resulting in significant reduction in specific capacitance at high mass loading.³⁵ Additionally, in conventional methods of preparation of these metal oxide-based nanocomposites films, binder material such as polytetrafluoroethylene (PTFE) needs to be added to improve the film stability. However, PTFE is insulating and reduces the electrical conductivity of the film. Therefore, if a binder material is highly conductive and can further disperse the densely packed MnO_2/CNTs bundles and stabilize them in solutions, it could solve the potential problem. PEDOT–PSS conducting polymer, which is water-soluble and can disperse carbon nanotubes and other nanomaterials in water, could be a good candidate for such a binder. In general, our strategy is shown schematically in Figure 1, where the MnO_2 nanospheres are directly grown on CNTs. In such a composite, MnO_2 offers the desired high specific capacitance and CNTs' framework provides the improved electrical conductivity and mechanical stability. However, the controlled growth of the right MnO_2 nanostructures on CNTs is not trivial. The synthesis processes are complicated when growing MnO_2 nanophase on CNTs surface, since the interfacial

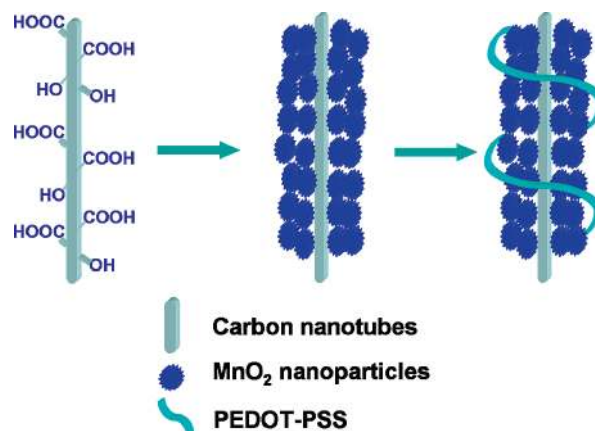


FIGURE 1. Sketch of $\text{MnO}_2/\text{CNTs}/\text{PEDOT-PSS}$ ternary composite.

chemistry may affect the nature of the deposited MnO_2 . Fortunately, sonochemical processing provided a method for such synthesis. It has proven to be a useful method for not only dispersing and functionalizing CNTs,^{36,37} but also to prepare mesoporous metal oxide.^{38,39} In the present study, we have explored a simple but efficient ultrasound-mediated coprecipitation method to prepare hierarchical MnO_2 nanosphere directly on well dispersed fFWNTs.

Furthermore, PEDOT–PSS is added in the composite and provides much needed functions. It acts not only as a dispersant to stabilize the composite suspension to facilitate the electrode film fabrication, but also offers good interparticle connectivity between the oxide material and the CNTs. Indeed, both CNTs and PEDOT–PSS are also involved in the charge storage process as conducting additives, both of which can contribute to the energy storage of the entire film. Thus, such a ternary composite is expected to offer much improved performance of the electrode film, which is often difficult to achieve from either the pristine hydrous MnO_2 or its binary composites such as PEDOT–PSS/ MnO_2 .

In this work, the $\text{MnO}_2/\text{fFWNTs}$ composites were synthesized using an efficient approach (see Supporting Information II). Briefly, FWNTs with high surface area⁴⁰ were first functionalized by acid treatment to attach carboxylic groups or hydroxyl groups on the sidewalls of the outer shell. Since the inner tube is protected by the outer shell, the electrical conductivity and structural integrity of the inner tubes remains superior. As can be seen from Figure 2A, the functionalized FWNTs still keep their intact structure after nitric acid treatment (see Supporting Information III). MnO_2 precursors (KMnO_4 and MnSO_4) were exposed to ultrasonic irradiation in the presence of modified FWNTs afterward at room temperature, leading to the formation of the hierarchical MnO_2 nanophere on fFWNTs mesoporous fFWNTs network (Figure 2A) within short time. The MnO_2 loading on fFWNTs can be controlled by tuning the ratio between fFWNTs and the MnO_2 precursors.

Figure 2C,D shows the morphology and microstructure of a representative composite with 60 wt % MnO_2 , 30 wt %

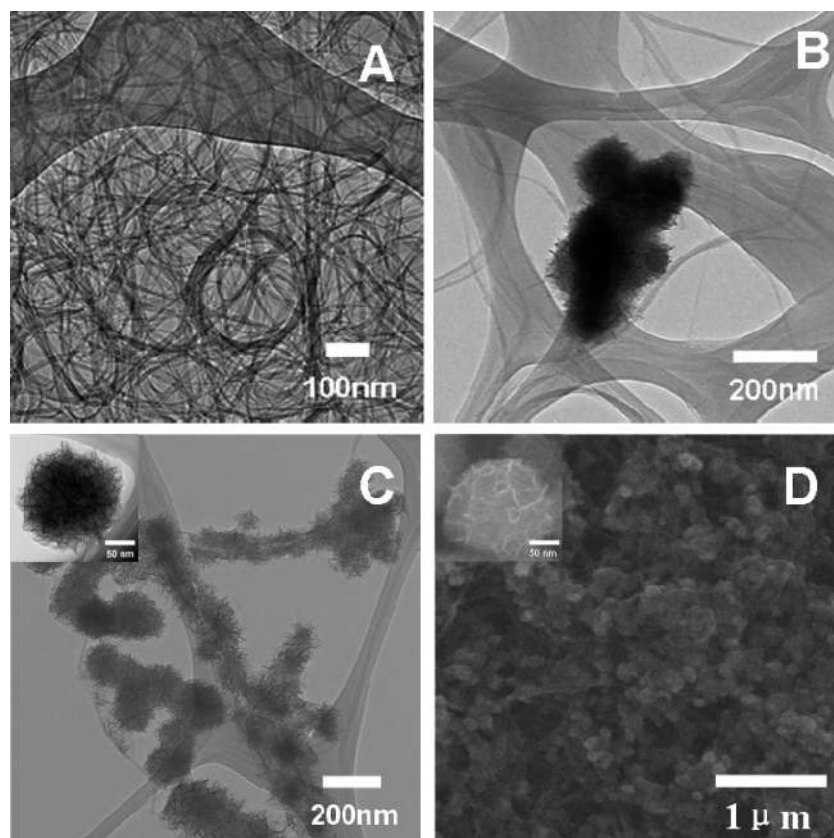


FIGURE 2. (A) TEM image of fFWNTs, (B) TEM image of direct mixing of MnO_2 nanospheres with fFWNTs, and (C) TEM and (D) SEM images of PEDOT–PSS dispersed MnO_2 nanospheres in situ grown on fFWNTs.

fFWNTs, and 10 wt % PEDOT–PSS. As can be seen in the figures, a unique hierarchical MnO_2 architecture has been successfully grown on a continuous functionalized FWNTs network. Evidently, MnO_2 nanosphere shows a tendency to have strong interaction with fFWNTs (Figure 2C) compared with the direct mixing of MnO_2 nanosphere with fFWNTs (Figure 2B). No aggregations of the MnO_2 nanoparticles off fFWNTs scaffold are observed in the composite, indicating that the nucleation is predominantly on the exterior surfaces of fFWNTs. Although the exact growth mechanism has not been completely understood, we suggest that oxygen-containing functional groups on fFWNTs can act as anchoring sites or nucleation sites for the growth of MnO_2 . The Mn^{2+} ions in the solution are preferentially adsorbed on these sites due to electrostatic force between Mn^{2+} ions and polar oxygen functional groups introduced by acid treatment. Subsequently, the Mn^{2+} ions are oxidized by KMnO_4 to form amorphous MnO_2 particles under ultrasonic irradiation. Additionally, transmission electron microscopy (TEM) image (Figure 2C) reveals that the MnO_2 nanospheres have uniform “crumpled paper ball” morphology (Figure 2C inset). SEM further confirms that MnO_2 exhibited an architecture with lots of small “wormholelike” pores size of 2–50 nm. (Figure 2D inset). Noticeably, those mesopores provide huge surface areas, enabling effective electrolyte transport and active-site accessibility. Additionally, the MnO_2 nano-

spheres are intertwined with both highly conductive fFWNTs and PEDOT–PSS, facilitating efficient electron transport. We also observed that electrodes prepared without PEDOT–PSS have large aggregations and can be easily peeled off from the current collector, indicating PEDOT–PSS works as not only the additional current collector, but also the binder material.

The two characteristic peaks at 37.1 and 66.3° in XRD analysis marked by an arrow in Figure 3A indicates the presence of MnO_2 , and the weak, broad signals suggest that MnO_2 is in amorphous nature, which is favorable for supercapacitor applications.⁴¹ The XPS spectrum (Figure 3B) acquired from MnO_2 /fFWNTs composite shows only signals from Mn, C, and O. The average manganese oxidation state was determined from the Mn 3s and O 1s core level spectra. On the basis of the analysis of Mn 3s spectrum,^{42,43} the manganese oxidation state is around 3.84 and the one obtained based on the analysis of O 1s spectrum⁴⁴ is 3.78. (see Supporting Information IV).

As we discussed earlier, CNTs serve both as electroactive material and as the scaffold for the deposition of the porous MnO_2 nanospheres, thus both of their surface area and electrical conductivity are critical for obtaining high performance. The ideal CNTs should have high surface area as well as high conductivity. Most of the times, these two properties do not exist together. Normally, to obtain high surface area,

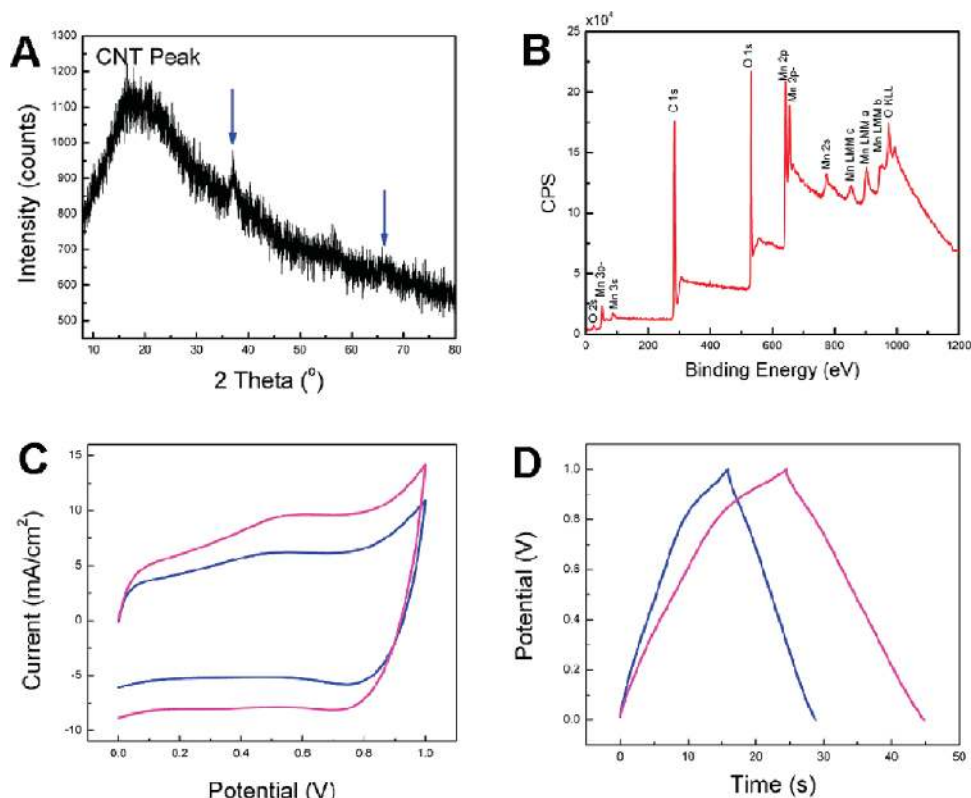


FIGURE 3. (A) XRD pattern and (B) XPS spectrum of the MnO₂/fFWNTs composite. (C) Cyclic voltammograms (500 mV/s scanned from 0–1 V in 1 M Na₂SO₄) and (D) Glavanostatic charge/discharge curves of MnO₂/fFWNT/PEDOT–PSS (pink) and MnO₂/fWNT/PEDOT–PSS (blue) composites at current densities of 1 mA/cm².

CNTs are functionalized with functional groups to improve suspension stability and to reduce the bundle size before the fabrication of composites.⁴⁵ However, electrical conductivity of CNTs decreases if too much functional groups are created on the sidewall of nanotubes. Therefore, to have both high capacitance and good rate performance, a proper balance between the specific surface area and the electrical conductivity must be achieved through well controlled functionalization steps. To investigate the chemical functionalization effect of carbon nanotubes on the electrochemical performance of electrodes by our functionalization method (see Supporting Information III), composite film electrodes with both purified and 6 M nitric acid functionalized nanotubes have been fabricated (see Supporting Information VI). Cyclic voltammograms (CV) (see Supporting Information VII) of those composites in 1 M Na₂SO₄ solution at very high scan rate of 500 mVs⁻¹ are depicted in Figure 3C. As can be seen from Figure 3C, composites with both purified FWNT and further functionalized FWNTs show rectangular CV curve, indicating both composite films are highly reversible as ideal capacitors. Calculations (see Supporting Information V) based on glavanostatic charge/discharge curves (Figure 3D) (see Supporting Information VII) indicated that films fabricated with functionalized FWNTs exhibit much higher specific capacitance (427 F/g) compared with the specific capacitance (381 F/g) of the film prepared with unfunctionalized FWNTs. It is believed that the good specific capaci-

tance of electrodes prepared with functionalized FWNTs is mainly due to the increased surface area and consistently high electrical conductivity. Furthermore, the enhanced hydrophilicity by functionalization not only facilitate the access of the electrolyte ions onto the fFWNTs surface but also improved the interaction between MnO₂ nanoparticles and fFWNTs making electron transport between fFWNTs and MnO₂ easier. Additionally, the high specific capacitance value confirms that the combination of all three types of the materials allows maximizing the utilization of manganese oxide.

To further explore the advantages of this novel design for real applications, we investigated the electrochemical properties of composite electrodes with high content of MnO₂ (60%) and fairly high mass loading (~1.5 mg/cm²) (see Supporting Information VI). As comparison, specific capacitance values of pure MnO₂ film, MnO₂/PEDOT–PSS composite film have also been tested. The MnO₂ nanospheres used for the comparison were synthesized with a similar method but without the addition of fFWNTs (Supporting Information II). As can be seen from Figure 4A, the severely distorted CV shape of pure MnO₂ film indicates its intrinsically poor electric conductivity. MnO₂/PEDOT–PSS binary composite show improved current than that of pure MnO₂ electrode under the same sweep speed, suggesting that conductive PEDOT–PSS facilitates the electron transport in the film. Surprisingly, the CV shape of the ternary composite

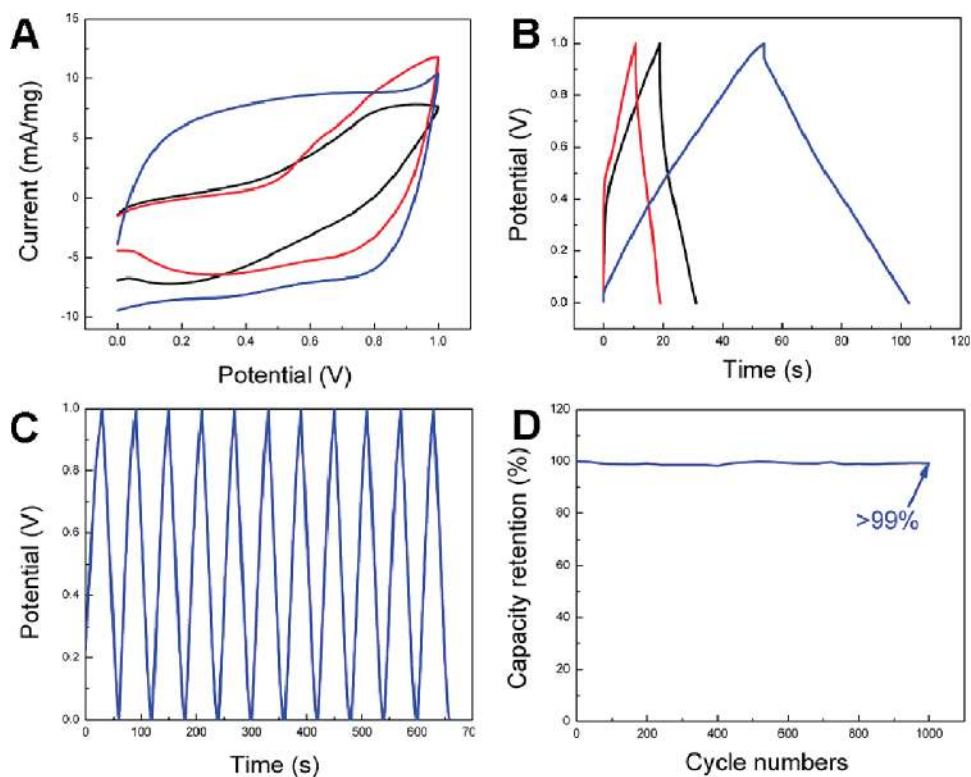


FIGURE 4. (A) Cyclic voltammograms (50 mV/s scanned from 0–1 V in 1 M Na₂SO₄) and (B) Galvanostatic charge/discharge curve (at current density of 5 mA/cm²) of MnO₂ film (black), MnO₂/PEDOT–PSS composite (red), and MnO₂/fFWNT/PEDOT–PSS ternary composite (blue). (C) Typical galvanostatic charge/discharge cycle curves of ternary composite electrodes obtained at current density of mA/cm². (D) Charge–discharge cycle test.

film of with even 60 wt % MnO₂ is nearly rectangular and its current value is much higher than that of pure MnO₂ film and MnO₂/PEDOT–PSS electrode. It implies that even at high concentration of MnO₂ and fairly high mass loading, the ternary composite exhibits the behavior closer to an ideal capacitor and the electrochemical utilization of MnO₂ has been greatly improved by the introduction of fFWNTs and PEDOT–PSS as “inner” and “outer” current collector. We are also glad to see the trend in specific capacitances calculated based on the galvanostatic charge/discharge curves in Figure 4B. As can be seen from the constant current charge–discharge curves, ternary composite shows ideal capacitive behavior with very sharp responses and small internal resistance (IR) drop. Specific capacitance of the ternary composite film reaches 200 F/g even at high concentration of MnO₂ (MnO₂, 60 wt %; fFWNTs, 30 wt %; PEDOT–PSS, 10 wt %) at current density of 5 mA/cm². Much lower specific capacitance is obtained for MnO₂ (129 F/g) and MnO₂/PEDOT–PSS (132 F/g). The improved high capacitance can be attributed to the optimized structure of the ternary composite. In a word, the combination of MnO₂, fFWNTs, and PEDOT–PSS into a single electrode showed excellent electrochemical performance for energy storage applications.

Long cycling life is an important requirement for supercapacitor electrodes. The cycling life test over 1000 cycles for the ternary composite electrode was carried out. Figure 4C dem-

onstrates the very stable charge–discharge cycles. Figure 4D illustrates that the nanocomposite electrodes showed only less than 1 % decay in available specific capacity after 1000 cycles. Charge–discharge cycle test of the ternary composite film suggests that the synergetic interaction among fFWNTs, MnO₂, and PEDOT–PSS significantly improved the electrical properties and the mechanical stability of the electrode.

Rate capability is another important factor for the use of supercapacitors in power applications. A good electrochemical energy storage device is required to provide its high energy density (or specific capacitance) at a high charge–discharge rate. The variation of specific capacitance of different MnO₂ electrodes with an increase in current density is shown in Figure 5. MnO₂/fFWNTs/PEDOT–PSS ternary composite not only exhibit high specific capacitance values but also maintain them well at high current density compared to other electrodes. As shown in Figure 5, the ternary composite preserved 85 % of its specific capacitance (from 200 to 168 F/g) as the current density increases from 5 to 25 mA/cm². However, the specific capacitance values of MnO₂ film (129 F/g) are not only much lower than the ternary composite but also decreased significantly with increased current densities (e.g., from 129 to 20 F/g at current density of 5–25 mA/cm²). Similar result was observed in MnO₂/PEDOT–PSS binary composite (e.g., from 132 to 37 F/g at current density of 5–25 mA/cm²). The superior rate capability in the ternary composites electrode

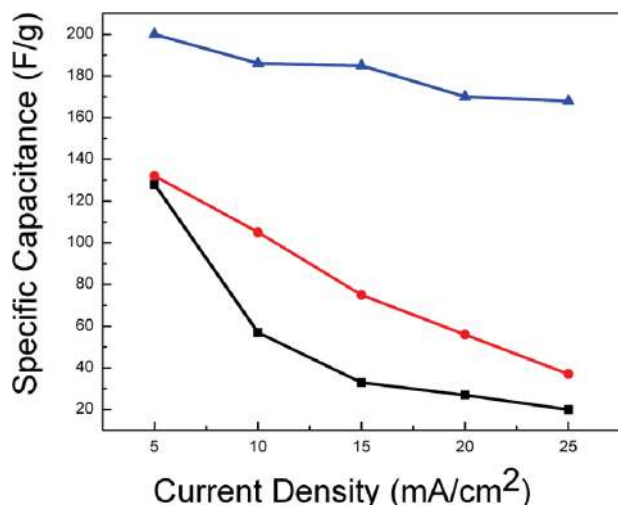


FIGURE 5. Specific capacitance of MnO₂/fFWNT/PEDOT-PSS ternary composite (blue), MnO₂/PEDOT-PSS composite (red), and MnO₂ film (black) at different charge/discharge current densities.

can be attributed to the reduced short diffusion path of ions, high surface area and increased electrical conductivity. Because of the synergetic contribution from fFWNTs and PEDOT-PSS, the high-surface area and porous network structure allows a higher rate of solution infiltration and facilitate the ions insertion/extraction and electrons transport in the electrode film. On the contrary, the severer aggregation, lower conductivity, and poor mechanical stability in MnO₂ film and MnO₂/PEDOT-PSS composite increased the ion diffusion and electron transport resistance, compromising their electrochemical performances.

In summary, a simple and cost-effective approach is developed to fabricate outstanding MnO₂/CNT/CP ternary nanocomposite. In such a composite, each component provide much needed critical function for efficient use of metal oxide for energy storage; fFWNTs not only provide high surface for the deposition of hierarchical MnO₂ porous nanospheres but also improve the electrical conductivity and the mechanical stability of the composite; PEDOT-PSS functions as an effective dispersant for MnO₂/fFWNTs structures and as binder material in improving the adhesion to the substrate and the connection among MnO₂/fFWNTs particles in the film; the highly porous MnO₂ nanospheres provide high surface area for improved specific capacitances. Working together, these components assemble into a mesoporous, interpenetrating network structure, which offers the composite with high specific capacitance, excellent rate capability, and long cycling life stability. We believe this design concept can be generalized toward other electrochemical materials containing metal oxides, such as RuO₂, Co₃O₄, and NiO, opening a new avenue for a large spectrum of device applications.

Acknowledgment. This work is supported by Duke University and by the National Science Foundation (NSF) and the Environmental Protection Agency (EPA) under NSF

Cooperative Agreement EF-0830093, Center for the Environmental Implications of NanoTechnology (CEINT). Any opinions, findings, conclusions, or recommendations expressed in this material are those of the author(s) and do not necessarily reflect the views of the NSF or the EPA. This work has not been subjected to EPA review and no official endorsement should be inferred. The authors also acknowledge the help by Professor Mark Weisner's group on electrochemical characterization and support from Duke SMIF (Share Materials Instrumentation Facilities).

Supporting Information Available. Experimental details, calculations, additional figures, and additional references. This material is available free of charge via the Internet at <http://pubs.acs.org>.

REFERENCES AND NOTES

- Zhang, L. L.; Zhao, X. S. Carbon-based materials as supercapacitor electrodes. *Chem. Soc. Rev.* **2009**, *38* (9), 2520–2531.
- Hu, L. B.; Choi, J. W.; Yang, Y.; Jeong, S.; La Mantia, F.; Cui, L. F.; Cui, Y. Highly conductive paper for energy-storage devices. *Proc. Natl. Acad. Sci. U.S.A.* **2009**, *106* (51), 21490–21494.
- Hulicova-Jurcakova, D.; Puziy, A. M.; Poddubnaya, O. I.; Suarez-Garcia, F.; Tascon, J. M. D.; Lu, G. Q. Highly Stable Performance of Supercapacitors from Phosphorus-Enriched Carbons. *J. Am. Chem. Soc.* **2009**, *131* (14), 5026.
- Kaempgen, M.; Chan, C. K.; Ma, J.; Cui, Y.; Gruner, G. Printable Thin Film Supercapacitors Using Single-Walled Carbon Nanotubes. *Nano Lett.* **2009**, *9* (5), 1872–1876.
- Fonseca, C. P.; Benedetti, J. E.; Neves, S. Poly(3-methyl thiophene)/PVDF composite as an electrode for supercapacitors. *J. Power Sources* **2006**, *158* (1), 789–794.
- Wang, H. L.; Hao, Q. L.; Yang, X. J.; Lu, L. D.; Wang, X. Graphene oxide doped polyaniline for supercapacitors. *Electrochem. Commun.* **2009**, *11* (6), 1158–1161.
- Hu, C. C.; Chang, K. H.; Lin, M. C.; Wu, Y. T. Design and tailoring of the nanotubular arrayed architecture of hydrous RuO₂ for next generation supercapacitors. *Nano Lett.* **2006**, *6* (12), 2690–2695.
- Cui, L.; Li, J.; Zhang, X. G. Preparation and properties of Co₃O₄ nanorods as supercapacitor material. *J. Appl. Electrochem.* **2009**, *39* (10), 1871–1876.
- Nam, K. W.; Lee, C. W.; Yang, X. Q.; Cho, B. W.; Yoon, W. S.; Kim, K. B. Electrodeposited manganese oxides on three-dimensional carbon nanotube substrate: Supercapacitive behaviour in aqueous and organic electrolytes. *J. Power Sources* **2009**, *188* (1), 323–331.
- Ko, J. M.; Kim, K. M. Electrochemical properties of MnO₂/activated carbon nanotube composite as an electrode material for supercapacitor. *Mater. Chem. Phys.* **2009**, *114* (2–3), 837–841.
- Tang, X. H.; Liu, Z. H.; Zhang, C. X.; Yang, Z. P.; Wang, Z. L. Synthesis and capacitive property of hierarchical hollow manganese oxide nanospheres with large specific surface area. *J. Power Sources* **2009**, *193* (2), 939–943.
- Luo, J. Y.; Cheng, L.; Xia, Y. Y. LiMn₂O₄ hollow nanosphere electrode material with excellent cycling reversibility and rate capability. *Electrochem. Commun.* **2007**, *9* (6), 1404–1409.
- Ra, W. Y.; Nakayama, M.; Uchimoto, Y.; Wakihara, M. Experimental and computational study of the electronic structural changes in LiTi₂O₄ spinel compounds upon electrochemical Li insertion reactions. *J. Phys. Chem. B* **2005**, *109* (3), 1130–1134.
- Ye, L. N.; Wu, C. Z.; Guo, W.; Xie, Y. MoS₂ hierarchical hollow cubic cages assembled by bilayers: one-step synthesis and their electrochemical hydrogen storage properties. *Chem. Commun.* **2006**, (45), 4738–4740.
- Wang, Y.; Su, F. B.; Lee, J. Y.; Zhao, X. S. Crystalline carbon hollow spheres, crystalline carbon-SnO₂ hollow spheres, and crystalline SnO₂ hollow spheres: Synthesis and performance in reversible Li-ion storage. *Chem. Mater.* **2006**, *18* (5), 1347–1353.
- Duan, G.; Cai, W.; Luo, Y.; Sun, F. A hierarchically structured Ni(OH)₂ monolayer hollow-sphere array and its tunable optical

- properties over a large region. *Adv. Funct. Mater.* **2007**, *17* (4), 644–650.
- (17) Xu, M.; Kong, L.; Zhou, W.; Li, H. Hydrothermal synthesis and pseudocapacitance properties of alpha-MnO₂ hollow spheres and hollow urchins. *J. Phys. Chem. C* **2007**, *111* (51), 19141–19147.
- (18) Luo, J.; Huang, A. M.; Park, S. H.; Suib, S. L.; O'Young, C. L. Crystallization of sodium-birnessite and accompanied phase transformation. *Chem. Mater.* **1998**, *10* (6), 1561–1568.
- (19) Hill, J. P.; Alam, S.; Ariga, K.; Anson, C. E.; Powell, A. K. Nanostructured microspheres of MnO₂ formed by room temperature solution processing. *Chem. Commun.* **2008**, (3), 383–385.
- (20) Zhang, H.; Cao, G. P.; Yang, Y. S. Carbon nanotube arrays and their composites for electrochemical capacitors and lithium-ion batteries. *Energy Environ. Sci.* **2009**, *2* (9), 932–943.
- (21) Pang, S. C.; Anderson, M. A.; Chapman, T. W. Novel electrode materials for thin-film ultracapacitors: Comparison of electrochemical properties of sol-gel-derived and electrodeposited manganese dioxide. *J. Electrochem. Soc.* **2000**, *147* (2), 444–450.
- (22) Obreja, V. V. N. On the performance of supercapacitors with electrodes based on carbon nanotubes and carbon activated material - A review. *Phys. E (Amsterdam, Neth.)* **2008**, *40* (7), 2596–2605.
- (23) Sivakkumar, S. R.; Ko, J. M.; Kim, D. Y.; Kim, B. C.; Wallace, G. G. Performance evaluation of CNT/polypyrrole/MnO₂ composite electrodes for electrochemical capacitors. *Electrochim. Acta* **2007**, *52* (25), 7377–7385.
- (24) Bordjiba, T.; Belanger, D. Direct Redox Deposition of Manganese Oxide on Multiscaled Carbon Nanotube/Microfiber Carbon Electrode for Electrochemical Capacitor. *J. Electrochem. Soc.* **2009**, *156* (5), A378–A384.
- (25) Zhang, H.; Cao, G. P.; Wang, Z. Y.; Yang, Y. S.; Shi, Z. J.; Gu, Z. N. Growth of manganese oxide nanoflowers on vertically-aligned carbon nanotube arrays for high-rate electrochemical capacitive energy storage. *Nano Lett.* **2008**, *8* (9), 2664–2668.
- (26) Yan, D.; Yan, P. X.; Yue, G. H.; Liu, J. Z.; Chang, J. B.; Yang, Q.; Qu, D. M.; Geng, Z. R.; Chen, J. T.; Zhang, G. A.; Zhuo, R. F. Self-assembled flower-like hierarchical spheres and nanobelts of manganese oxide by hydrothermal method and morphology control of them. *Chem. Phys. Lett.* **2007**, *440* (1–3), 134–138.
- (27) Zheng, H. J.; Tang, F. Q.; Jia, Y.; Wang, L. Z.; Chen, Y. C.; Lim, M.; Zhang, L.; Lu, G. Q. Layer-by-layer assembly and electrochemical properties of sandwiched film of manganese oxide nanosheet and carbon nanotube. *Carbon* **2009**, *47* (6), 1534–1542.
- (28) Ma, S. B.; Nam, K. W.; Yoon, W. S.; Yang, X. Q.; Ahn, K. Y.; Oh, K. H.; Kim, K. B. Electrochemical properties of manganese oxide coated onto carbon nanotubes for energy-storage applications. *J. Power Sources* **2008**, *178* (1), 483–489.
- (29) Hu, L. B.; Pasta, M.; La Mantia, F.; Cui, L. F.; Jeong, S.; Deshazer, H. D.; Choi, J. W.; Han, S. M.; Cui, Y. Stretchable, Porous, and Conductive Energy Textiles. *Nano Lett.* **2010**, *10* (2), 708–714.
- (30) Liu, R.; Lee, S. B. MnO₂/Poly(3,4-ethylenedioxythiophene) coaxial nanowires by one-step coelectrodeposition for electrochemical energy storage. *J. Am. Chem. Soc.* **2008**, *130* (10), 2942–2945.
- (31) Liu, F. J. Electrodeposition of manganese dioxide in three-dimensional poly(3,4-ethylenedioxythiophene)-poly(styrene sulfonic acid)-polyaniline for supercapacitor. *J. Power Sources* **2008**, *182* (1), 383–388.
- (32) Sun, L. J.; Liu, X. X. Electrodepositions and capacitive properties of hybrid films of polyaniline and manganese dioxide with fibrous morphologies. *Eur. Polym. J.* **2008**, *44* (1), 219–224.
- (33) Fischer, A. E.; Pettigrew, K. A.; Rolison, D. R.; Stroud, R. M.; Long, J. W. Incorporation of homogeneous, nanoscale MnO₂ within ultraporous carbon structures via self-limiting electroless deposition: Implications for electrochemical capacitors. *Nano Lett.* **2007**, *7* (2), 281–286.
- (34) Qian, C.; Qi, H.; Gao, B.; Cheng, Y.; Qiu, Q.; Qin, L. C.; Zhou, O.; Liu, J. Fabrication of small diameter few-walled carbon nanotubes with enhanced field emission property. *J. Nanosci. Nanotechnol.* **2006**, *6* (5), 1346–1349.
- (35) Staiti, P.; Lufitano, F. Study and optimization of manganese oxide-based electrodes for electrochemical supercapacitors. *J. Power Sources* **2009**, *187* (1), 284–289.
- (36) Chen, H. Y.; Jacobs, O.; Wu, W.; Rudiger, G.; Schadel, B. Effect of dispersion method on tribological properties of carbon nanotube reinforced epoxy resin composites. *Polym. Test.* **2007**, *26* (3), 351–360.
- (37) Zhang, W.; Yang, M. J. Dispersion of carbon nanotubes in polymer matrix by in-situ emulsion polymerization. *J. Mater. Sci.* **2004**, *39* (15), 4921–4922.
- (38) Zolfaghari, A.; Ataherian, F.; Ghaemi, M.; Gholami, A. Capacitive behavior of nanostructured MnO₂ prepared by sonochemistry method. *Electrochim. Acta* **2007**, *52* (8), 2806–2814.
- (39) Srivastava, D. N.; Perkas, N.; Zaban, A.; Gedanken, A. Sonochemistry as a tool for preparation of porous metal oxides. *Pure Appl. Chem.* **2002**, *74* (9), 1509–1517.
- (40) Hou, Y.; Tang, J.; Zhang, H. B.; Qian, C.; Feng, Y. Y.; Liu, J. Functionalized Few-Walled Carbon Nanotubes for Mechanical Reinforcement of Polymeric Composites. *ACS Nano* **2009**, *3* (5), 1057–1062.
- (41) Bao, S. J.; He, B. L.; Liang, Y. Y.; Zhou, W. J.; Li, H. L. Synthesis and electrochemical characterization of amorphous MnO₂ for electrochemical capacitor. *Mater. Sci. Eng., A* **2005**, *397* (1–2), 305–309.
- (42) Chigane, M.; Ishikawa, M. Manganese oxide thin film preparation by potentiostatic electrolyses and electrochromism. *J. Electrochem. Soc.* **2000**, *147* (6), 2246–2251.
- (43) Chigane, M.; Ishikawa, M.; Izaki, M. Preparation of manganese oxide thin films by electrolysis/chemical deposition and electrochromism. *J. Electrochem. Soc.* **2001**, *148* (7), D96–D101.
- (44) Toupin, M.; Brousse, T.; Belanger, D. Charge storage mechanism of MnO₂ electrode used in aqueous electrochemical capacitor. *Chem. Mater.* **2004**, *16* (16), 3184–3190.
- (45) Pan, H.; Li, J. Y.; Feng, Y. P. Carbon Nanotubes for Supercapacitor. *Nanoscale Res. Lett.* **2010**, *5* (3), 654–668.